

# SUPPORTING INFORMATION

## Efficient Near-UV Emitters Based on Cationic Bis-Pincer Iridium(III) Carbene Complexes

*Noviyan Darmawan,<sup>1,2,†</sup> Cheng-Han Yang,<sup>2</sup> Matteo Mauro,<sup>2,†</sup> Matthieu Raynal,<sup>3</sup> Susanne Heun,<sup>4</sup> Junyou Pan,<sup>4</sup> Herwig Buchholz,<sup>4</sup> Pierre Braunstein,<sup>3</sup> and Luisa De Cola<sup>2,†,\*</sup>*

1. NRW Graduate School of Chemistry, University of Münster, Germany.

2. Physikalisches Institut and CeNTech, University of Münster, Heisenbergstrasse 11, D-48149  
Münster, Germany.

<sup>†</sup> Current address: Institut de Science et d'Ingénierie Supramoléculaires, UMR 7006, Université de Strasbourg, 8 allée Gaspard Monge, F-67083 Strasbourg (France). E-mail: decola@unistra.fr

3. Laboratoire de Chimie de Coordination, Institut de Chimie, UMR 7177 CNRS, Université de Strasbourg, 4 rue Blaise Pascal, F-67081 Strasbourg Cedex, France .

4. Merck KGaA, Frankfurterstrasse 250, D-64293 Darmstadt, Germany.

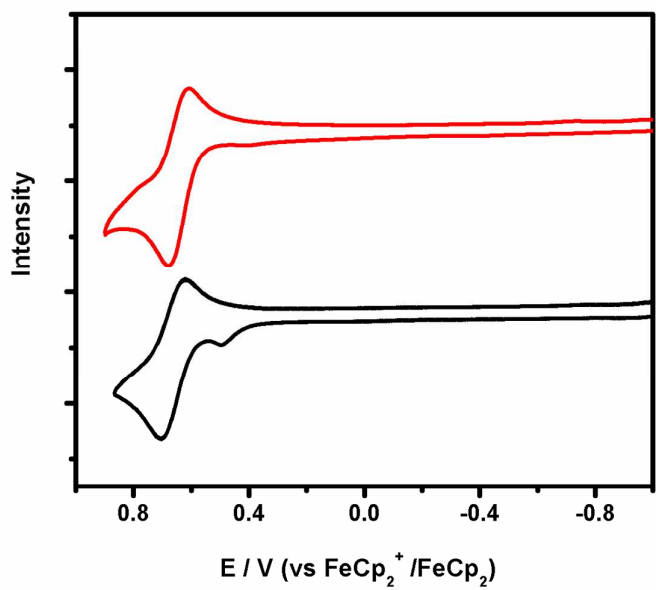


**Figure S1.** Electrochemical profile of complexes **1·I** (black) and **1·PF<sub>6</sub>** (red). The reported values are relative to  $\text{FeCp}_2^+ | \text{FeCp}_2$ . Scan rate 100 mV s<sup>-1</sup>.

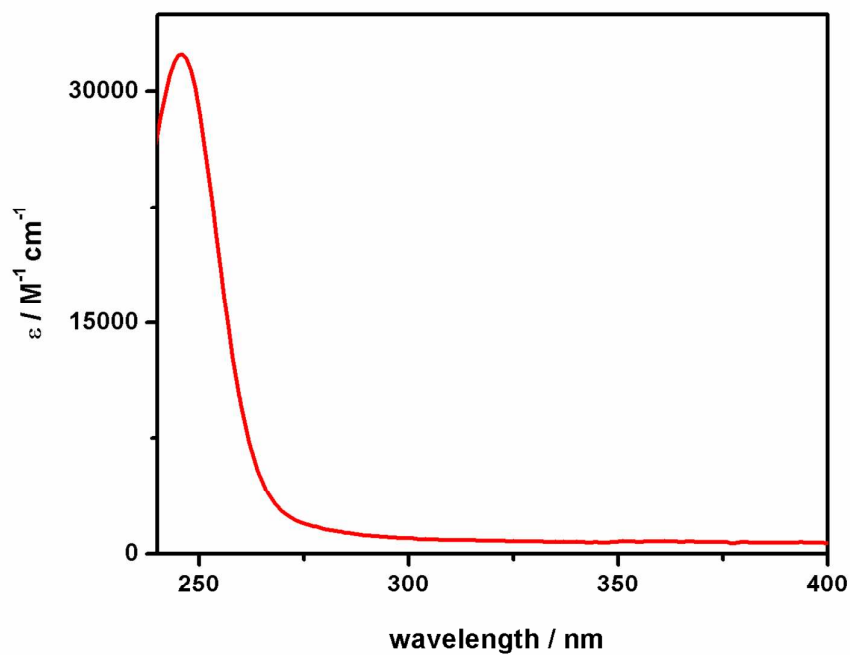


**Figure S2.** Absorption spectrum of the free <sup>nBu</sup>(C<sub>NHC</sub><sup>Me</sup>CC<sub>NHC</sub>)<sub>2</sub> ligand (room temperature, CH<sub>3</sub>CN).

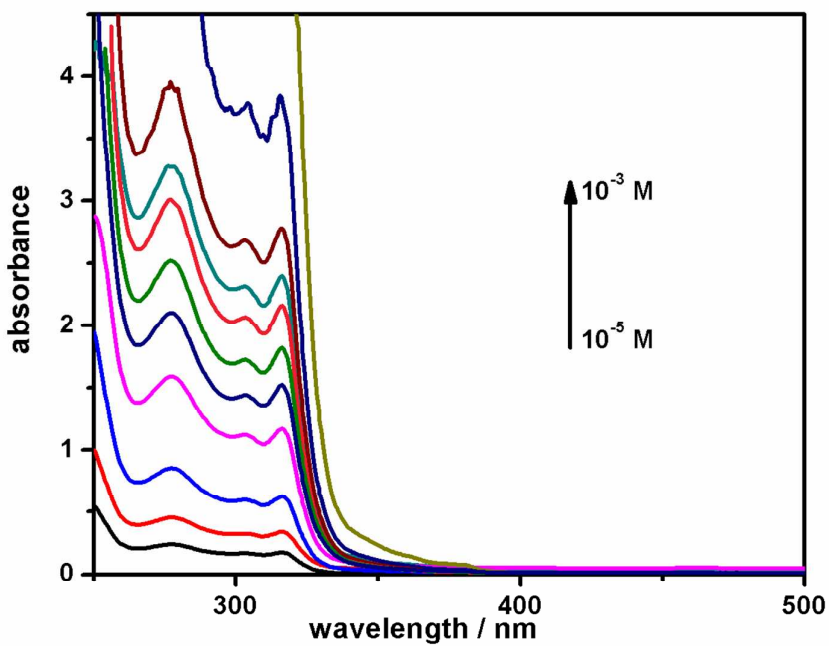


**Figure S3.** Absorption spectra of different concentrations ( $10^{-5}$  to  $10^{-3}$  M) of **1**·I in acetonitrile (298 K).

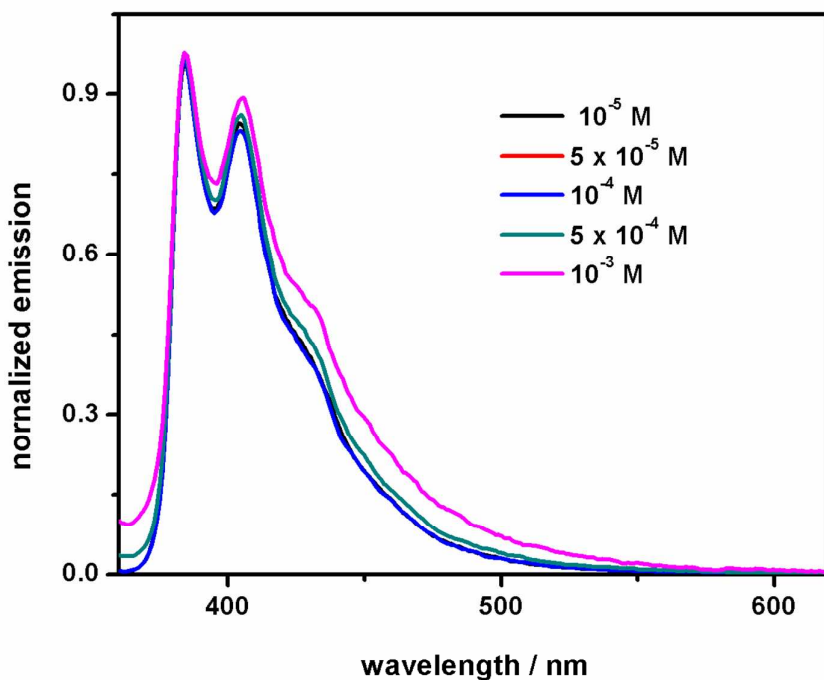


**Figure S4.** Emission spectra of different concentrations of **1**·I in acetonitrile (298K).

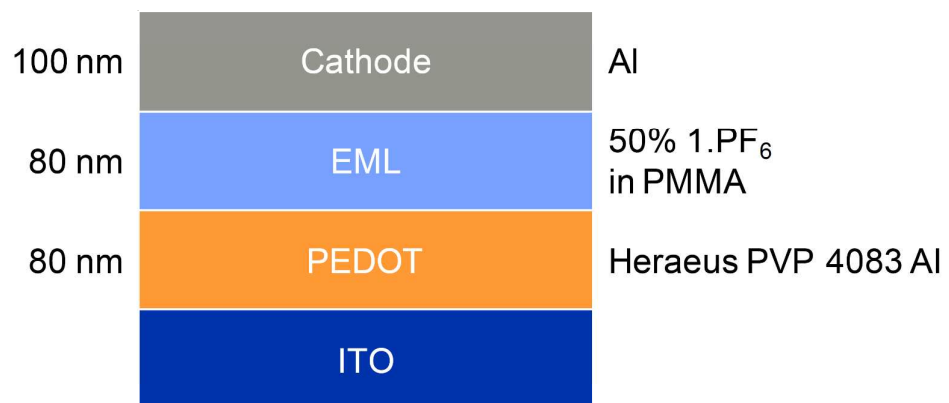


**Figure S5.** Schematic view of the near-UV electroluminescent device.

**Table S1.** Crystallographic data and structure refinement for **1·PF<sub>6</sub>**.

Empirical formula	C44 H58 F6 Ir N8 P
Formula weight	1036.15
Temperature	173(2) K
Wavelength	0.71073 Å
Crystal system, space group	Monoclinic, P 21/c
Unit cell dimensions	$a = 15.9489(6)$ Å   alpha = 90 deg. $b = 14.1730(5)$ Å   beta = 112.109(2) deg. $c = 25.0561(8)$ Å   gamma = 90 deg.
Volume	5247.3(3) Å <sup>3</sup>
Z, Calculated density	4, 1.312 Mg/m <sup>3</sup>
Absorption coefficient	2.631 mm <sup>-1</sup>
F(000)	2096
Crystal size	0.25 x 0.20 x 0.15 mm
Theta range for data collection	1.96 to 29.99 deg.
Limiting indices	-20<=h<=22, -19<=k<=19, -34<=l<=35
Reflections collected / unique	45512 / 15222 [R(int) = 0.0355]
Completeness to theta = 29.99	99.5 %
Absorption correction	Semi-empirical from equivalents
Max. and min. transmission	0.6936 and 0.5591
Refinement method	Full-matrix least-squares on $F^2$
Data / restraints / parameters	15222 / 0 / 549
Goodness-of-fit on $F^2$	1.027
Final R indices [I>2sigma(I)]	R1 = 0.0381, wR2 = 0.0874
R indices (all data)	R1 = 0.0613, wR2 = 0.0941
Largest diff. peak and hole	3.584 and -1.328 e.Å <sup>-3</sup>

**Table S2.** Selected geometrical parameters [ $\text{\AA}$ ,  $^\circ$ ] and energy [ $E_{\text{h}}$ ]<sup>a</sup> of the optimized ground state optimized geometry for the complex  $[\text{Ir}^{\text{Me}}(\text{C}_{\text{NHC}}^{\text{Me}}\text{CC}_{\text{NHC}})_2]^+$ , **2**. A partial atom-labelling scheme is reported in Figure 4.

bond	length [ $\text{\AA}$ ]	angle	amplitude [ $^\circ$ ]
$R(\text{Ir}(1)-\text{C}(1))$	2.084	$\angle(\text{C}(2)-\text{Ir}(1)-\text{C}(27))$	76.32
$R(\text{Ir}(1)-\text{C}(27))$	2.061	$\angle(\text{Ir}(1)-\text{C}(2)-\text{N}(12))$	115.72
$R(\text{C}(2)-\text{N}(3))$	1.357	$\angle(\text{C}(2)-\text{N}(12)-\text{C}(13))$	117.50
$R(\text{N}(3)-\text{C}(4))$	1.459	$\phi\text{N}(12)-\text{C}(2)-\text{Ir}(1)-\text{C}(38))$	0.00
$R(\text{N}(3)-\text{C}(8))$	1.390	$\phi\text{N}(12)-\text{C}(2)-\text{Ir}(1)-\text{C}(39))$	103.31
$R(\text{C}(8)-\text{C}(10))$	1.356	$\phi\text{N}(12)-\text{C}(2)-\text{Ir}(1)-\text{C}(27))$	0.00
$R(\text{C}(10)-\text{N}(12))$	1.390	-	-
$R(\text{N}(12)-\text{C}(13))$	1.434	-	-
$R(\text{C}(13)-\text{C}(27))$	1.396	-	-
Energy		-1782.205255	

<sup>a</sup> 1  $E_{\text{h}} = 2625.500 \text{ kJ mol}^{-1}$

**Table S3.** List of selected molecular orbital energies for the complex  $[\text{Ir}^{\text{Me}}(\text{C}_{\text{NHC}}^{\text{Me}}\text{CC}_{\text{NHC}})_2]^+$ , **2**, and HOMO–LUMO energy gap in gas phase, given in eV. For each entry, the symmetry of the corresponding orbital is also reported in parenthesis.

orbital	energy	orbital	energy
LUMO + 10 (e)	-1.470	HOMO (b <sub>1</sub> )	-7.735
LUMO + 9 (e)	-1.470	HOMO - 1 (e)	-7.736
LUMO + 8 (a <sub>2</sub> )	-1.528	HOMO - 2 (e)	-7.736
LUMO + 7 (b <sub>1</sub> )	-1.558	HOMO - 3 (a <sub>2</sub> )	-8.179
LUMO + 6 (e)	-1.682	HOMO - 4 (e)	-8.607
LUMO + 5 (e)	-1.682	HOMO - 5 (e)	-8.607
LUMO + 4 (a <sub>1</sub> )	-2.329	HOMO - 6 (b <sub>1</sub> )	-8.617
LUMO + 3 (e)	-2.532	HOMO - 7 (b <sub>2</sub> )	-8.764
LUMO + 2 (e)	-2.532	HOMO - 8 (a <sub>2</sub> )	-9.170
LUMO + 1 (b <sub>1</sub> )	-2.746	HOMO - 9 (e)	-9.744
LUMO (a <sub>2</sub> )	-2.823	HOMO - 10 (e)	-9.744
HOMO–LUMO gap		4.912	

**Table S4.** Computed excitation energies and oscillator strengths for the  $S_0 \rightarrow S_n$  ( $n = 1\text{--}30$ ) and of the five lowest  $S_0 \rightarrow T_m$  ( $m = 1\text{--}5$ ) (where  $m = 1\text{--}5$ ) transitions of the complex  $[\text{Ir}^{\text{Me}}(\text{C}_{\text{NHC}}^{\text{Me}}\text{CC}_{\text{NHC}})_2]^+$ , **2**, at its ground state ( $S_0$ ) optimized geometry. The calculations were performed in gas phase and acetonitrile, the latter by using the IEFPCM solvation model. Only calculated excitations with  $f \geq 0.02$  and single excitation configurations with higher contributions are listed, along with the corresponding symmetry.

$\lambda$ [nm, eV] ( $f$ ) <sup>a</sup> (symmetry) expansion coefficient	gas phase		acetonitrile (IEFPCM)	
	$S_0 \rightarrow S_n$	$S_0 \rightarrow T_m$	$S_0 \rightarrow S_n$	$S_0 \rightarrow T_m$
289, 4.284 (0.075) ( $S_1$ ) (E)	371, 3.339 (0.000) ( $T_1$ ) ( ${}^3\text{B}_2$ )	290, 4.273 (0.101) ( $S_1$ ) (E)	370, 3.348 (0.000) ( $T_1$ ) ( ${}^3\text{B}_2$ )	
0.313 HOMO - 2 → LUMO	0.360 HOMO - 3 → LUMO + 1	-0.312 HOMO - 2 → LUMO	0.360 HOMO - 3 → LUMO + 1	
-0.479 HOMO - 2 → LUMO + 1	0.389 HOMO → LUMO	0.440 HOMO - 2 → LUMO + 1	0.390 HOMO → LUMO	
0.302 HOMO - 1 → LUMO + 1		0.337 HOMO - 1 → LUMO + 1		
289, 4.284 (0.075) (E)	371, 3.343 (0.000) ( $T_2$ ) ( ${}^3\text{A}_1$ )	290, 4.273 (0.101) (E)	370, 3.351 (0.000) ( $T_2$ ) ( ${}^3\text{A}_1$ )	
0.302 HOMO - 2 → LUMO + 1	0.371 HOMO - 3 → LUMO	-0.337 HOMO - 2 → LUMO + 1	0.371 HOMO - 3 → LUMO	
0.313 HOMO - 1 → LUMO	0.390 HOMO → LUMO + 1	0.312 HOMO - 1 → LUMO	0.391 HOMO → LUMO + 1	
0.479 HOMO - 1 → LUMO + 1		0.440 HOMO - 1 → LUMO + 1		
282, 4.398 (0.094) ( ${}^1\text{B}_2$ )	333, 3.724 (0.000) ( $T_3$ ) (E)	285, 4.357 (0.153) ( ${}^1\text{B}_2$ )	332, 3.729 (0.000) ( $T_3$ ) (E)	
0.668 HOMO → LUMO	0.463 HOMO - 2 → LUMO	0.684 HOMO → LUMO	0.464 HOMO - 1 → LUMO	
	0.482 HOMO - 2 → LUMO + 1		0.482 HOMO - 1 → LUMO + 1	
270, 4.584 (0.135) (E)	333, 3.724 (0.000) ( $T_4$ ) (E)	270, 4.591 (0.186) (E)	332, 3.729 (0.000) ( $T_4$ ) (E)	
0.474 HOMO - 2 → LUMO + 2	-0.463 HOMO - 1 → LUMO	0.485 HOMO - 2 → LUMO + 2	-0.464 HOMO - 2 → LUMO	
0.472 HOMO - 1 → LUMO + 3	0.482 HOMO - 1 → LUMO + 1	0.485 HOMO - 1 → LUMO + 3	0.482 HOMO - 2 → LUMO + 1	
250, 4.953 (0.189) ( ${}^1\text{B}_2$ )	320, 3.876 (0.000) ( $T_5$ ) (E)	251, 4.942 (0.252) ( ${}^1\text{B}_2$ )	320, 3.874 (0.000) ( $T_5$ ) ( ${}^3\text{A}_1$ )	
0.671 HOMO - 3 → LUMO + 1	0.374 HOMO - 2 → LUMO + 3	0.677 HOMO → LUMO + 1	-0.373 HOMO - 2 → LUMO + 2	
	-0.374 HOMO - 1 → LUMO + 2		0.373 HOMO - 1 → LUMO + 3	
248, 5.009 (0.025) (E)		244, 5.087 (0.027) (E)	320, 3.874 (0.000) ( $T_5$ ) ( ${}^3\text{A}_1$ )	
0.613 HOMO - 3 → LUMO + 3		0.254 HOMO - 5 → LUMO	-0.373 HOMO - 2 → LUMO + 2	
248, 5.009 (0.025) (E)		0.330 HOMO - 5 → LUMO + 1	0.373 HOMO - 1 → LUMO + 3	
0.613 HOMO - 3 → LUMO + 2		0.483 HOMO - 3 → LUMO + 2	0.379 HOMO → LUMO + 1	
232, 5.329 (0.021) ( ${}^1\text{B}_2$ )		233, 5.315 (0.051) ( ${}^1\text{B}_2$ )		
0.517 HOMO - 6 → LUMO		0.548 HOMO - 6 → LUMO		

<sup>a</sup> TD-DFT calculations performed with Gaussian09 neglect intersystem crossing processes, which mix states of the singlet and triplet manifolds. For this reason, the computed oscillator strengths for triplet excitation transitions are equal to zero.

**Table S5.** Computed excitation energies and oscillator strengths for the  $S_0 \rightarrow S_n$  ( $n = 1\text{--}5$ ) and of the five lowest  $S_0 \rightarrow T_m$  ( $m = 1\text{--}3$ ) transitions of the complex **1** $\cdot$ PF<sub>6</sub> at its ground state ( $S_0$ ) geometry derived from the X-ray crystal structure. The calculations were performed in gas phase and acetonitrile, the latter by using the IEFPCM solvation model. Only calculated excitations with  $f \geq 0.02$  and single excitation configurations with higher contributions are listed. All the computed transitions have A symmetry.

	<i>gas phase</i>		<i>acetonitrile (IEFPCM)</i>	
	$S_0 \rightarrow S_n$	$S_0 \rightarrow T_m$	$S_0 \rightarrow S_n$	$S_0 \rightarrow T_m$
$\lambda$ [nm, eV] ( $f$ ) <sup>a</sup> (symmetry) expansion coefficient	296, 4.189 (0.008) ( $S_1$ ) 0.588 HOMO $\rightarrow$ LUMO 0.215 HOMO - 1 $\rightarrow$ LUMO	361, 3.435 (0.000) ( $T_1$ ) 0.363 HOMO $\rightarrow$ LUMO -0.291 HOMO - 7 $\rightarrow$ LUMO	287, 4.318 (0.035) ( $S_1$ ) 0.487 HOMO $\rightarrow$ LUMO 0.427 HOMO $\rightarrow$ LUMO + 1	359, 3.455 (0.000) ( $T_1$ ) -0.354 HOMO - 3 $\rightarrow$ LUMO 0.330 HOMO - 1 $\rightarrow$ LUMO
	290, 4.279 (0.025) ( $S_2$ ) 0.493 HOMO $\rightarrow$ LUMO + 1 0.314 HOMO - 1 $\rightarrow$ LUMO	359, 3.455 (0.000) ( $T_2$ ) 0.350 HOMO - 5 $\rightarrow$ LUMO + 1 0.318 HOMO $\rightarrow$ LUMO + 1	285, 4.346 (0.079) ( $S_2$ ) 0.483 HOMO $\rightarrow$ LUMO + 1 -0.365 HOMO $\rightarrow$ LUMO	357, 3.469 (0.000) ( $T_2$ ) -0.318 HOMO - 3 $\rightarrow$ LUMO + 1 -0.293 HOMO $\rightarrow$ LUMO + 1
	289, 4.283 (0.027) ( $S_3$ ) 0.468 HOMO - 2 $\rightarrow$ LUMO 0.358 HOMO - 1 $\rightarrow$ LUMO	329, 3.773 (0.000) ( $T_3$ ) 0.612 HOMO - 2 $\rightarrow$ LUMO -0.223 HOMO - 1 $\rightarrow$ LUMO	283, 4.384 (0.069) ( $S_3$ ) 0.514 HOMO - 2 $\rightarrow$ LUMO 0.296 HOMO - 1 $\rightarrow$ LUMO	324, 3.825 (0.000) ( $T_3$ ) 0.515 HOMO $\rightarrow$ LUMO + 1 -0.398 HOMO - 1 $\rightarrow$ LUMO + 1
	285, 4.343 (0.088) ( $S_4$ ) 0.410 HOMO - 1 $\rightarrow$ LUMO -0.404 HOMO - 2 $\rightarrow$ LUMO		280, 4.429 (0.035) ( $S_4$ ) 0.369 HOMO - 1 $\rightarrow$ LUMO + 1 -0.346 HOMO $\rightarrow$ LUMO + 2	
	283, 4.374 (0.052) ( $S_5$ ) 0.429 HOMO - 1 $\rightarrow$ LUMO + 1 0.391 HOMO - 2 $\rightarrow$ LUMO + 1			

<sup>a</sup> TD-DFT calculations performed with Gaussian09 neglect intersystem crossing processes, which mix states of the singlet and triplet manifolds. For this reason, the computed oscillator strengths for triplet excitation transitions are equal to zero.

